

Upper limits from HESS active galactic nuclei observations in 2005–2007

F. Aharonian^{1,13}, A. G. Akhperjanian², U. Barres de Almeida^{8,*}, A. R. Bazer-Bachi³, B. Behera¹⁴, M. Beilicke⁴, W. Benbow¹, K. Bernlöhr^{1,5}, C. Boisson⁶, O. Bolz¹, V. Borrel³, I. Braun¹, E. Brion⁷, A. M. Brown⁸, R. Bühler¹, T. Bulik²⁴, I. Büsching⁹, T. Boutelier¹⁷, S. Carrigan¹, P. M. Chadwick⁸, L.-M. Chounet¹⁰, A. C. Clapson¹, G. Coignet¹¹, R. Cornils⁴, L. Costamante^{1,28}, M. Dalton⁵, B. Degrange¹⁰, H. J. Dickinson⁸, A. Djannati-Atai¹², W. Domainko¹, L. O’C. Drury¹³, F. Dubois¹¹, G. Dubus¹⁷, J. Dyks²⁴, K. Egberts¹, D. Emmanoulopoulos¹⁴, P. Espigat¹², C. Farnier¹⁵, F. Feinstein¹⁵, A. Fiasson¹⁵, A. Förster¹, G. Fontaine¹⁰, S. Funk⁵, M. Füßling⁵, Y. A. Gallant¹⁵, B. Giebels¹⁰, J. F. Glicenstein⁷, B. Glück¹⁶, P. Goret⁷, C. Hadjichristidis⁸, D. Hauser¹, M. Hauser¹⁴, G. Heinzlmann⁴, G. Henri¹⁷, G. Hermann¹, J. A. Hinton²⁵, A. Hoffmann¹⁸, W. Hofmann¹, M. Holleran⁹, S. Hoppe¹, D. Horns¹⁸, A. Jacholkowska¹⁵, O. C. de Jager⁹, I. Jung¹⁶, K. Katarzyński²⁷, E. Kendziorra¹⁸, M. Kerschhaggl⁵, B. Khélifi¹⁰, D. Keogh⁸, Nu. Komin¹⁵, K. Kosack¹, G. Lamanna¹¹, I. J. Latham⁸, A. Lemièrè¹², M. Lemoine-Goumard¹⁰, J.-P. Lenain⁶, T. Lohse⁵, J. M. Martin⁶, O. Martineau-Huynh¹⁹, A. Marcowith¹⁵, C. Masterson¹³, D. Maurin¹⁹, G. Maurin¹², T. J. L. McComb⁸, R. Moderski²⁴, E. Moulin⁷, M. de Naurois¹⁹, D. Nedbal²⁰, S. J. Nolan⁸, S. Ohm¹, J.-P. Olive³, E. de Oña Wilhelmi¹², K. J. Orford⁸, J. L. Osborne⁸, M. Ostrowski²³, M. Panter¹, G. Pedalletti¹⁴, G. Pelletier¹⁷, P.-O. Petrucci¹⁷, S. Pita¹², G. Pühlhofer¹⁴, M. Punch¹², S. Ranchon¹¹, B. C. Raubenheimer⁹, M. Raue⁴, S. M. Rayner⁸, M. Renaud¹, J. Ripken⁴, L. Rob²⁰, L. Rolland⁷, S. Rosier-Lees¹¹, G. Rowell²⁶, B. Rudak²⁴, J. Ruppel²¹, V. Sahakian², A. Santangelo¹⁸, R. Schlickeiser²¹, F. Schöck¹⁶, R. Schröder²¹, U. Schwanke⁵, S. Schwarzburg¹⁸, S. Schwemmer¹⁴, A. Shalchi²¹, H. Sol⁶, D. Spangler⁸, Ł. Stawarz²³, R. Steenkamp²², C. Stegmann¹⁶, G. Superina¹⁰, P. H. Tam¹⁴, J.-P. Tavernet¹⁹, R. Terrier¹², C. van Eldik¹, G. Vasileiadis¹⁵, C. Venter⁹, J. P. Vialle¹¹, P. Vincent¹⁹, M. Vivier⁷, H. J. Völk¹, F. Volpe¹⁰, S. J. Wagner¹⁴, M. Ward⁸, A. A. Zdziarski²⁴, and A. Zech⁶

(Affiliations can be found after the references)

Received 3 September 2007 / Accepted 6 November 2007

ABSTRACT

Aims. Very high energy (VHE; $E > 100$ GeV) γ -ray studies were performed for 18 active galactic nuclei (AGN) from a variety of AGN classes. **Methods.** VHE observations of a sample of 14 AGN, considered candidate VHE emitters, were made with the High Energy Stereoscopic System (HESS) between January 2005 and July 2007. Large-zenith-angle observations of three northern AGN (Mkn 421, Mkn 501, 1ES 1218+304), known to emit VHE γ -rays, were also performed in order to sample their spectral energy distributions (SEDs) above 1 TeV. In addition, the VHE flux from 1ES 1101–232, previously detected by HESS in 2004–2005, was monitored during 2006 and 2007.

Results. As significant detections from the HESS observation program are reported elsewhere, the results reported here are primarily integral flux upper limits. The average exposure for each of the 14 VHE-candidate AGN is ~ 7 h live time, and the observations have an average energy threshold between 230 GeV and 590 GeV. Upper limits for these 14 AGN range from $<0.9\%$ to $<4.9\%$ of the Crab Nebula flux, and eight of these are the most constraining ever reported for the object. The brief (<2.2 h each) large-zenith-angle observations yield upper limits for Mkn 501 ($<20\%$ Crab above 2.5 TeV) and 1ES 1218+304 ($<17\%$ Crab above 1.0 TeV), and a marginal detection (3.5σ) of Mkn 421 (50% Crab above 2.1 TeV). 1ES 1101–232 was marginally detected (3.6σ , 1.7% Crab above 260 GeV) during the 2006 (13.7 h live time) observations, but not in the 2007 (4.6 h live time) data. The upper limit in 2007 ($<1.9\%$ Crab above 260 GeV) is below the average flux measured by HESS from 2004–2006.

Key words. galaxies: active – gamma rays: observations

1. Introduction

Active galactic nuclei (AGN) represent the only class of extragalactic objects known to emit VHE γ -rays. These objects are found in the core of at least 5% of all galaxies. Generally, they are characterized by very bright, highly variable, non-thermal emission spanning the entire electromagnetic spectrum from

radio waves to TeV γ -rays. They are believed to be powered by accretion of matter onto a super-massive (10^6 – 10^9 solar mass) black hole. In the unified description of AGN (as reviewed in Urry & Padovani 1995), this black hole is surrounded in the inner regions by an accretion disk, and in the outer regions by a thick torus of gas and dust. Viewing these objects at various orientation angles with respect to the torus plane is believed to be the underlying cause of the wide variations in their observed properties, and hence numerous AGN classifications.

* Supported by CAPES Foundation, Ministry of Education of Brazil.

Table 1. Ten AGN detected by HESS in order of redshift (z).

AGN ^a	z	Reference
M 87	0.004	Aharonian et al. (2006e)
Mkn 421	0.030	Aharonian et al. (2005c)
PKS 0548-322*	0.069	Superina et al. (2007)
PKS 2005-489*	0.071	Aharonian et al. (2005b)
PKS 2155-304 [†]	0.116	Aharonian et al. (2005a)
1ES 0229+200*	0.139	Aharonian et al. (2007d)
H 2356-309* [†]	0.165	Aharonian et al. (2006c)
1ES 1101-232* [†]	0.186	Aharonian et al. (2007a)
1ES 0347-121*	0.188	Aharonian et al. (2007c)
PG 1553+113* [†]	?	Aharonian et al. (2006a)

^a The asterisk denotes the seven AGN which were discovered to emit VHE γ -rays by HESS. The dagger marks the objects with more than one HESS publication.

In about 10% of all AGN, collimated relativistic outflows of particles (known as relativistic jets) exist, presumably along the magnetic field in the vicinity of the black hole, and approximately perpendicular to the accretion disk and torus plane. Of particular interest to high-energy astronomy is a class of radio-loud AGN known as blazars which includes both BL Lacertae (BL Lac) type objects and Flat Spectrum Radio Quasars (FSRQ). For blazars, one relativistic jet is pointed close the observer's line-of-sight (i.e. towards Earth), causing the observed emission to be relativistically beamed. Blazars are typically characterized by a double-peaked broad-band SED, and for different objects the peak energy of the lower or higher-energy components can differ by several orders of magnitude. BL Lac objects are commonly categorized (Padovani & Giommi 1995) into three groups depending on the position of the first peak: low (LBL), intermediate (IBL), and high-frequency-peaked (HBL). Essentially all¹ AGN detected at VHE energies are HBL.

The HESS array (Hinton 2004; Aharonian et al. 2006d) of four imaging atmospheric-Cherenkov telescopes located in Namibia is used to search for VHE γ -ray emission from various classes of astrophysical objects. Approximately 30% of the HESS observation program is dedicated to studies of AGN, primarily blazars. Since 2005, the ~ 300 h per year of AGN observations are divided between monitoring known VHE-bright AGN for bright flaring episodes, and searching for new VHE sources. For the discovery part of the AGN program, a candidate from a large, diverse sample of relatively nearby AGN is typically observed for ~ 10 h. If any of these observations show an indication for a signal (e.g., an excess with significance more than ~ 3 standard deviations), a deeper exposure is promptly scheduled to increase the overall significance of the detection and to allow for a spectral measurement. The detections resulting from the HESS AGN observation program are reported elsewhere (see Table 1 for references). Results of HESS AGN observations taken from January 2005 through July 2007, where VHE emission is not significantly detected, are presented here.

2. Methodology

The HESS AGN data presented here were generally taken in ~ 28 min data segments (runs) using *Wobble* mode, where the pointing of the array is slightly offset, typically² by $\pm 0.5^\circ$, from

¹ Out of the ~ 20 VHE AGN, the only published exceptions are the radio galaxy M 87 (Aharonian et al. 2003, 2006e) and BL Lacertae (Albert et al. 2007) (an LBL). See Sect. 3.1 for more details.

² For the only exception, BWE 0210+1159, the average offset is $\sim 0.9^\circ$.

the position of the AGN. For the results reported in this article, all HESS data passing the quality-selection criteria³ are processed using the standard HESS calibration (Aharonian et al. 2004) and analysis tools (Benbow 2005). The *standard cuts* (Benbow 2005) are chosen for the event-selection criteria. On-source data are taken from a circular region of radius $\theta_{\text{cut}} = 0.11^\circ$, appropriate for point-like sources, centered on each AGN. The *Reflected-Region* method (Berge et al. 2007) is used to simultaneously estimate the cosmic-ray background (off-source data). Equation (17) in Li & Ma (1983) is used to calculate the significance (in standard deviations, σ) of the observed excess. All upper limits are determined following the method of Feldman & Cousins (1998). The flux limits in Sect. 3.2 are all calculated assuming a power-law spectrum with photon index $\Gamma = 3.0$ as none of these targets are previously detected in the VHE regime. The limits are not very sensitive to the choice of photon index. Assuming a moderately different photon index (i.e. Γ between 2.5 and 3.5) changes the values by less than $\sim 10\%$. Even the choice of an extremely soft spectrum ($\Gamma = 6.0$) increases the limits by only $\sim 25\%$. The fluxes and limits in Sects. 4 and 5 assume spectra previously measured for those sources. All flux quantities and energy thresholds are corrected for decreases over time of the absolute optical efficiency of the system, using efficiencies determined from simulated and observed muons (Aharonian et al. 2006d). Therefore the energy thresholds of these AGN observations are higher than that of the newly commissioned HESS system reported in Benbow (2005) as the total optical throughput is between $\sim 25\%$ to $\sim 35\%$ less than initially measured in 2003. The integral flux quantities given later are compared to the HESS Crab Nebula flux calculated above the energy threshold determined for each AGN respectively. The reported percentages of the HESS Crab Nebula flux are calculated from the fit to HESS spectrum (Aharonian et al. 2006d) and assume that the function does not deviate from a power-law below the lowest energy measured (~ 500 GeV).

3. HESS observations of 14 AGN

Approximately 30 AGN were observed by HESS from January 2005 through July 2007. Some of these objects were previously shown by HESS to emit VHE γ -rays, and the discoveries of VHE emission from others are reported elsewhere. Of the remaining AGN with non-zero good-quality exposure, 14 show no indication of any VHE emission. Table 2 shows these 14 candidate AGN observed by HESS and the dates of the observations. The total live time of the observations passing the standard data-quality selection criteria, and the mean zenith angle of those observations, are listed in Table 3. The mean good-quality exposure for the candidates is 6.7 h live time at a mean zenith angle of 31° . In 5 h of observations, the sensitivity of HESS (Benbow 2005) enables a 5σ detection of a $\sim 2\%$ Crab Nebula flux source at 20° zenith angle. The sensitivity of HESS decreases at larger zenith angles. For example, in 5 h of observations at 45° zenith angle, a $\sim 3.5\%$ Crab Nebula flux source is detected at 5σ .

3.1. The 14 candidates

A large majority of VHE-emitting AGN are HBL, therefore these objects are the primary targets of HESS AGN observation program. However, prominent examples of different types

³ Approximately 70% of the relevant HESS AGN data pass these criteria.

Table 2. The candidate AGN ordered by right ascension in groups of blazars and non-blazars.

Object ^{a,b}	α_{J2000} [h m s]	δ_{J2000} [d m s]	z	Type	MJD–50000 ^c
<i>Blazar</i>					
III Zw 2	00 10 31.0	+10 58 30	0.0893	FSRQ	3944, 3953, 4267, 4270, 4272, 4274–76, 4278
BWE 0210+116 ^E	02 13 05.0	+12 13 06	0.250	LBL	3966–69, 3971, 3974, 3976–78
1ES 0323+022	03 26 14.0	+02 25 15	0.147	HBL	3668–69, 3676–78, 3998–4000
PKS 0521–365 ^E	05 22 58.0	–36 27 31	0.0553	LBL	4079–4081
3C 273 ^E	12 27 06.8	+02 03 09	0.158	FSRQ	3411, 3413, 3494–95, 3497, 3499, 3502, 3505, 4146–49, 4151, 4153, 4228–31
3C 279 ^E	12 56 11.2	–05 47 22	0.536	FSRQ	4118–4121
RBS 1888	22 43 42.0	–12 31 06	0.226	HBL	3914, 3916–18
HS 2250+1926 ^E	22 53 07.4	+19 42 35	0.284	FSRQ	4292–4302, 4304–05
PKS 2316–423	23 19 05.9	–42 06 49	0.055	IBL	3919–23
1ES 2343–151	23 45 37.8	–14 49 10	0.226	IBL	3592–95, 3597
<i>Non-blazar</i>					
NGC 1068	02 42 40.8	–00 00 48	0.00379	Sy II	4022, 4024, 4032
Pictor A	05 19 49.7	–45 46 45	0.0342	FR II	4051–54, 4056–57, 4060–64
PKS 0558–504	05 59 46.8	–50 26 39	0.137	NLS I	4110–4113, 4115–16, 4121
NGC 7469	23 03 15.8	+08 52 26	0.0164	Sy I	4020–21, 4023–24, 4032

^a The coordinates (J2000), redshift, and type (HBL, IBL, LBL, FSRQ, Sy = Seyfert (I & II), FR II = Fanaroff-Riley II, NLS I = Narrow-line Seyfert I) shown are taken from the SIMBAD Astronomical Database (<http://simbad.u-strasbg.fr/simbad/>) and the NASA/IPAC Extragalactic Database (<http://nedwww.ipac.caltech.edu/>).

^b The superscript E denotes the five candidates detected by the EGRET instrument aboard the CGRO satellite (Mukherjee et al. 1997; Hartman et al. 1999; Sowards-Emmerd et al. 2003).

^c Only the dates of the good-quality HESS observations of each AGN are shown.

of AGN are also observed. Many of the HBL observed by HESS have been detected, therefore the 14 candidates discussed in this section are largely not HBL.

3.1.1. Blazars

Only two of the 14 candidates are HBL. The HBL 1ES 0323+022 is the only target recommended by multiple authors (Stecker et al. 1996; Perlman 1999; Costamante & Ghisellini 2002) as a potential source of VHE γ -rays. The remaining blazar targets include two IBL, five AGN (2 LBL and 3 FSRQ) detected by EGRET (Mukherjee et al. 1997; Hartman et al. 1999; Sowards-Emmerd et al. 2003), and a high-frequency-peaked FSRQ. Although the lower-energy SED peaks of the other blazars might imply that they are less likely to emit VHE γ -rays, an LBL (the archetype BL Lacertae) was recently detected (Albert et al. 2007) by the MAGIC Collaboration.

3.1.2. Non-blazars

Only one non-blazar AGN, hosted by the radio-loud Fanaroff-Riley (FR) I galaxy M 87, has been detected (Aharonian et al. 2003, 2006e) at VHE energies. Of the four non-blazar targets, two (Pictor A and PKS 0558–504) are radio-loud objects and two (NGC 1068 and NGC 7469) are radio-weak. Pictor A, an FR II galaxy (Perley et al. 1997), is somewhat similar to a blazar, however its jet is oriented at a large angle with respect to the line-of-sight from Earth. Therefore the VHE flux from Pictor A is naively expected to be low, as any emission would not be Doppler-boosted along the line of sight. PKS 0558–504, a narrow-line Seyfert I galaxy, shows some evidence for beamed emission from a relativistic jet (Komossa et al. 2006). Detection of VHE emission from PKS 0558–504 would strongly support the presence of such a jet. The radio-weak objects observed by HESS do not have relativistic jets. They include the brightest and closest Seyfert II

object (NGC 1068), and a Seyfert I (NGC 7469) undergoing massive star formation near its nucleus (Genzel et al. 1995). It should be noted that VHE observations of non-blazar AGN have the potential to detect VHE emission originating from sites other than jets (e.g., hot-spots in radio lobes) and from mechanisms other than inverse-Compton scattering (e.g., proton acceleration in the vicinity of accreting black holes).

3.2. Results

No significant excess of VHE γ -rays is found from any of the 14 AGN in the given exposure time. The total good-quality live time (T), mean zenith angle of observation (Z_{obs}), number of on-source and off-source counts, off-source normalization, observed excess, and significance (S) of the excess in standard deviations are given for each of the 14 AGN in Table 3. Figure 1 shows the distribution of the significance observed from the direction of each of the 14 AGN. The distribution is slightly skewed towards positive values. However, combining the excess from all 14 candidates only yields a total of 54 events and a statistical significance of 0.8σ . A search for serendipitous source discoveries in the HESS field-of-view centered on each of the AGN also yields no significant excess.

Table 3 shows 99.9% confidence level (c.l.) upper limits on the integral flux (I) above the energy threshold of the observations (E_{th}) and the corresponding percentage of the HESS Crab Nebula flux. The systematic error on a HESS integral flux measurement is estimated to be $\sim 20\%$, and it is not included in the calculation of the upper limits.

A search for VHE flares from each observed AGN was also performed. Here the nightly integral flux above the average energy threshold was calculated from the observed excess and fit by a constant. Table 2 shows the dates each AGN was observed and Table 3 shows the resulting χ^2 probability $P(\chi^2)$. As each χ^2 probability is acceptable, no evidence for any VHE flares is found.

Table 3. Results from HESS observations of 14 AGN.

Object ^a	T [h]	Z_{obs} [°]	On	Off	Norm	Excess	S [σ]	E_{th} [GeV]	$I(>E_{\text{th}})$ [$10^{-12} \text{ cm}^{-2} \text{ s}^{-1}$]	Crab %	$P(\chi^2)$
<i>Blazars</i>											
III Zw 2 ^U	4.9	38	169	1801	0.0916	4	0.3	430	<2.14	<2.7	0.19
BWE 0210+116 ^U	6.0	43	176	3752	0.0504	-13	-0.9	530	<0.72	<1.2	0.74
1ES 0323+022	7.2	27	321	3302	0.0932	13	0.7	300	<2.52	<1.9	0.59
PKS 0521-365 ^U	3.1	26	180	1818	0.0928	11	0.8	310	<5.40	<4.2	0.45
3C 273 ^U	16.5	29	848	8678	0.0932	39	1.3	300	<1.97	<1.4	0.89
3C 279 ^U	2.0	26	100	1012	0.0942	5	0.5	300	<3.98	<2.9	0.44
RBS 1888	2.4	15	184	1625	0.0949	30	2.2	240	<9.26	<4.9	0.39
HS 2250+1926 ^U	17.5	44	597	6536	0.0923	-6	-0.2	590	<0.45	<0.9	0.58
PKS 2316-423	4.1	20	299	2910	0.0929	29	1.6	270	<4.74	<3.0	0.58
1ES 2343-151 ^U	8.6	17	557	6286	0.0911	-16	-0.6	230	<2.45	<1.2	0.67
<i>Non-blazar</i>											
NGC 1068	1.8	29	75	687	0.0955	9	1.1	330	<5.76	<4.9	0.47
Pictor A	7.9	31	397	4501	0.0932	-23	-1.1	320	<2.45	<2.0	0.54
PKS 0558-504 ^U	8.3	28	426	4740	0.0929	-14	-0.7	310	<2.38	<1.8	0.80
NGC 7469	3.4	34	98	1234	0.0909	-14	-1.3	330	<1.38	<1.2	0.59

^a The superscript U marks the eight VHE upper limits (99.9% c.l.) that are the most constraining ever published for the corresponding objects.

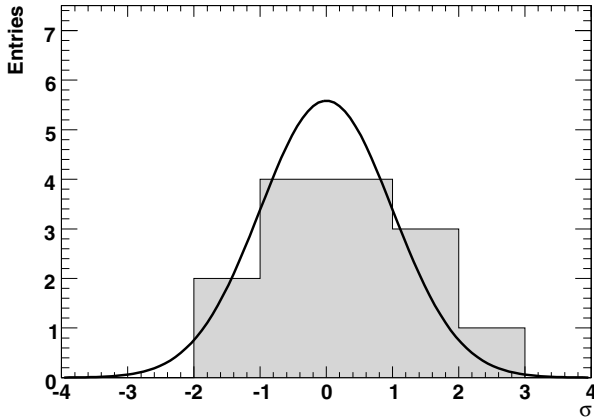


Fig. 1. Distribution of the significances observed from the 14 candidate AGN. The curve represents a Gaussian distribution with zero mean and a standard deviation of one.

4. Low altitude observations of VHE AGN

As HESS is located in the Southern Hemisphere, AGN with declinations greater than 30° culminate at low altitudes ($<37^\circ$) where the energy threshold of HESS is considerably higher and the sensitivity is reduced. However, due to the large effective area of the HESS array at low altitudes, observations of northern AGN probe higher energies than typically studied by Northern Hemisphere instruments. Simultaneous observations of the same target by both Northern and Southern Hemisphere instruments sample different parts of the VHE spectrum, potentially increasing the spectral coverage to several orders of magnitude and allowing for cross-calibration between the detectors (see, e.g., Mazin et al. 2005). Therefore, three northern AGN, known to emit VHE γ -rays, were briefly (good-quality live time <2.2 h) observed at low altitudes with HESS. For two of these targets (1ES 1218+304 and Mkn 501) simultaneous observations were performed by the MAGIC VHE telescope and the Suzaku X-ray satellite (Mitsuda et al. 2007).

4.1. Mkn 421

HESS observed the well-known VHE emitter (Punch et al. 1992) Mkn 421 on April 12, 2005 from 21:01 to 22:00 UTC. Both of the two 28-min runs pass the standard quality selection criteria, yielding a data set of 0.9 h live time at a mean zenith angle of 63° . A total of 81 on-source events, 873 off-source events, with an on-off normalization $\alpha = 0.0607$ are measured. A marginal excess (28 events, 3.5σ) is found. The corresponding integral flux above the 2.1 TeV analysis threshold is $I(>2.1 \text{ TeV}) = (3.4 \pm 1.2_{\text{stat}} \pm 0.7_{\text{syst}}) \times 10^{-12} \text{ cm}^{-2} \text{ s}^{-1}$, or 50% of the HESS Crab Nebula flux. The flux in each run differs by only 3%, clearly consistent within statistical errors. As the spectrum of Mkn 421 above 2 TeV is known to vary along with its flux (Aharonian et al. 2005c), the flux calculated here assumes the time-averaged spectrum, a power law with photon index $\Gamma = 2.39$ and an exponential cut-off at 3.6 TeV, measured (Aharonian et al. 2002) up to 10 TeV by HEGRA between December 1999 and May 2000 during a state of comparable flux.

4.2. 1ES 1218+304

1ES 1218+304, discovered as a VHE emitter by the MAGIC collaboration (Albert et al. 2006), was the target of a HESS observation campaign on May 19–21, 2006. All data from the first two nights of observations fail the data-quality criteria due to bad weather. On the last night, a total of five good-quality observation runs were taken between 17:43 and 21:05 UTC yielding a data set of 1.8 h live time at a mean zenith angle of 56° . One of the telescopes was not functioning properly during the data taking and is excluded from the analysis, resulting in a slightly reduced sensitivity. A total of 61 on-source events and 590 off-source events ($\alpha = 0.0880$) pass the event selection criteria. The resulting excess is not significant (9 events, 1.2σ). Assuming $\Gamma = 3.0$, as measured (Albert et al. 2006) by MAGIC from ~ 100 GeV to ~ 600 GeV, the 99.9% c.l. limit on the integral flux above the 1.0 TeV analysis threshold is $I(>1.0 \text{ TeV}) < (3.9 \pm 0.8_{\text{syst}}) \times 10^{-12} \text{ cm}^{-2} \text{ s}^{-1}$. This corresponds to 17% of the HESS Crab Nebula flux. The upper limit is ~ 6 times higher than the flux above 1 TeV determined from an extrapolation of the MAGIC spectrum.

Table 4. Results from HESS observations of 1ES 1101–232 during various observation epochs.

Epoch	On	Off	Norm	Excess	S [σ]	$I(>260 \text{ GeV})^a$ [$10^{-12} \text{ cm}^{-2} \text{ s}^{-1}$]
2006	1016	9803	0.0917	117	3.6	$2.8 \pm 0.7_{\text{stat}}$
2007	309	3220	0.0909	16	0.9	<3.1
Total	1325	13023	0.0915	133	3.6	$2.0 \pm 0.6_{\text{stat}}$
Suzaku	323	2938	0.0927	51	2.9	$3.2 \pm 1.4_{\text{stat}}$

^a The systematic error on the integral flux above 260 GeV is 20%. The 99.9% confidence limit is given for the 2007 observations.

4.3. Mkn 501

HESS observations of Mkn 501 (Quinn et al. 1996) occurred on July 18, 2006 from 18:49 to 21:18 UTC. All five 28-min runs pass the standard quality-selection criteria, yielding a data set of 2.2 h live time at a mean zenith angle of 64° . A total of 112 on-source events and 1328 off-source events ($\alpha = 0.0915$) are measured. Mkn 501 is not detected by HESS as the resulting excess is -9 events (-0.8σ). Assuming $\Gamma = 2.6$ as measured (Bradbury et al. 1997) above 1.5 TeV by HEGRA, the limit (99.9% c.l.) on the integral flux above the 2.5 TeV analysis threshold is $I(>2.5 \text{ TeV}) < (1.0 \pm 0.2_{\text{sys}}) \times 10^{-12} \text{ cm}^{-2} \text{ s}^{-1}$, or 20% of the HESS Crab Nebula flux.

5. VHE Monitoring of 1ES 1101–232

1ES 1101–232 was discovered by HESS (Aharonian et al. 2006b, 2007a) to emit VHE γ -rays during observations in 2004–2005. As part of a campaign to monitor its VHE flux, it was re-observed for 17.4 h between December 29, 2005 and May 28, 2006, and for 6.4 h from April 9–17, 2007. A total of 18.3 h, 13.7 h in 2006 and 4.6 h in 2007, pass the data-quality criteria. In addition, the Suzaku X-ray satellite observed 1ES 1101–232 from 16:07 UTC on May 25, 2006 until 05:11 UTC on May 27, 2006, with an average observation efficiency of $\sim 47\%$. (Suzaku Observation Log: <http://www.astro.isas.ac.jp/suzaku/index.html>. en). A total of 4.3 h of good-quality HESS data are simultaneous to the Suzaku observations. The results from the HESS observations are given in Table 4 for the various observation epochs. The number of on-source and off-source counts, the off-source normalization, the observed excess, the significance (S) of the excess in standard deviations, and the integral flux above the analysis threshold of 260 GeV are shown in the table. The object is marginally detected in the 2006 observations, as well as during the Suzaku epoch. 1ES 1101–232 is not detected in 2007. All flux quantities in Table 4 assume the photon index $\Gamma = 2.94$ previously measured (Aharonian et al. 2007a) by HESS for 1ES 1101–232.

There is no indication of significant variability in the VHE flux from 1ES 1101–232 within the 2006 or 2007 data, as the nightly flux within each year is well fit by a constant. Figure 2 shows a light curve of the integral flux above 260 GeV in annual bins for the observations here, as well as those previously published for the 2004–2005 data (Aharonian et al. 2007a). The 99.9% confidence limit on the integral flux in 2007 is marginally inconsistent with the average value, $I(>260 \text{ GeV}) = (3.50 \pm 0.35) \times 10^{-12} \text{ cm}^{-2} \text{ s}^{-1}$, measured by HESS from 2004–2006.

6. Discussion

One of the defining characteristics of AGN is their extreme variability. The VHE flux from any of these AGN may increase

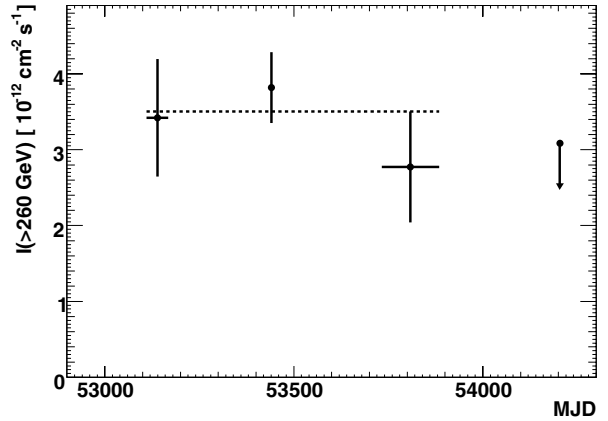


Fig. 2. Integral flux ($>260 \text{ GeV}$) measured by HESS from 1ES 1101–232 in annual bins. The 2004 and 2005 data were previously published (Aharonian et al. 2007a). The horizontal error bars reflect the actual observation dates (first to last observation in each period). The dashed line is the average flux measured from 2004–2006. The upper limit in 2007 is at the 99.9% confidence level.

significantly during future flaring episodes (see, e.g., Aharonian et al. 2007b) and could potentially exceed the limits presented here. In addition, accurate modeling of the SED requires that the state of the source is accounted for. Therefore it must be emphasized that the upper limits reported here constrain the flux of the AGN only during the observation time (see Table 2 for the 14 candidates). The simultaneous Suzaku X-ray data from Mkn 501, 1ES 1218+304, and 1ES 1101–232, make the HESS results from these objects particularly useful. In the absence of simultaneous observations at lower energies, it is recommended that the limits be conservatively interpreted as limits on the steady-component or quiescent flux from the AGN.

Interpretation of the SED of an AGN not only requires accounting for the state of the source, but also the redshift and energy dependent absorption (Gould & Schröder 1967) of VHE photons on the Extragalactic Background Light (EBL). The EBL density (Hauser & Dwek 2001; Aharonian et al. 2006b), and hence optical depth (τ), is only roughly constrained at wavelengths relevant to the HESS measurements. Therefore the effect of the EBL on the HESS limits is quantified with a maximal and minimal EBL density (i.e. maximal and minimal EBL absorption). Here the EBL parameterization of Primack et al. (2005) is used. This EBL is near the lower limits on the EBL density provided by galaxy counts (Madau & Pozzetti 2000) and is considered a minimal EBL scenario. Scaling the normalization of the minimal EBL parameterization by a factor of 1.6 yields a density approximately at the level of the most-constraining upper limits (Aharonian et al. 2006b) derived from VHE observations of 1ES 1101–232, and is therefore used here as a maximal EBL parameterization. Table 5 shows the HESS integral flux limits from Table 3 converted to a limit on

Table 5. Differential flux upper limits from the HESS observations.

Object	z	E_{th} [TeV]	F_{obs}^a [$10^{-11} \text{ cm}^{-2} \text{ s}^{-1} \text{ TeV}^{-1}$]	A_{Min}	A_{Max}
<i>VHE blazars</i>					
1ES 1218+304	0.182	1.0	<0.78	4.29	10.3
Mkn 501	0.0336	2.5	<0.064	1.43	1.76
<i>Blazars</i>					
III Zw 2	0.0893	0.43	<1.00	1.34	1.61
BWE 0210+116	0.250	0.53	<0.27	3.39	7.06
1ES 0323+022	0.147	0.30	<1.68	1.37	1.65
PKS 0521–365	0.0553	0.31	<3.48	1.12	1.20
3C 273	0.158	0.30	<1.31	1.40	1.72
3C 279	0.536	0.30	<2.65	5.12	13.7
RBS 1888	0.226	0.24	<7.72	1.46	1.83
HS 2250+1926	0.284	0.59	<0.15	4.88	12.6
PKS 2316–423	0.055	0.27	<3.51	1.09	1.16
1ES 2343–151	0.226	0.23	<2.13	1.42	1.76
<i>Non-blazar</i>					
NGC 1068	0.00379	0.33	<3.49	1.01	1.01
Pictor A	0.0342	0.32	<1.53	1.07	1.12
PKS 0558–504	0.137	0.31	<1.54	1.35	1.62
NGC 7469	0.0164	0.33	<0.84	1.04	1.06

^a The observed (F_{obs}) differential flux upper limits at the energy threshold of the HESS observations (E_{th}) are calculated at the 99.9% confidence level. The limit on the intrinsic differential flux is given by multiplying the observed limit by the scaling factor, $A = e^{\tau}$, for either a minimal (A_{Min}) or maximal (A_{Max}) EBL scenario.

the observed differential flux (F_{obs}) at the energy threshold of the HESS measurement, as well as scaling factors, $A = e^{\tau}$, to convert each to an intrinsic flux limit (i.e. correct for absorption) for both the minimal and maximal EBL scenarios. The corresponding information for the HESS limits on 1ES 1218+304 and Mkn 501 are also shown in Table 5. For Mkn 421 ($z = 0.030$) the differential flux at 2.1 TeV is $F_{\text{obs}} = (5.7 \pm 1.9_{\text{stat}} \pm 1.1_{\text{syst}}) \times 10^{-12} \text{ cm}^{-2} \text{ s}^{-1} \text{ TeV}^{-1}$, and the minimal and maximal scaling factors are $A_{\text{Min}} = 1.36$ and $A_{\text{Max}} = 1.63$, respectively. During the Suzaku epoch for 1ES 1101–232 ($z = 0.186$) the differential flux at 0.26 TeV is $F_{\text{obs}} = (2.4 \pm 1.0_{\text{stat}} \pm 0.5_{\text{syst}}) \times 10^{-11} \text{ cm}^{-2} \text{ s}^{-1} \text{ TeV}^{-1}$, and the minimal and maximal scaling factors are $A_{\text{Min}} = 1.40$ and $A_{\text{Max}} = 1.72$, respectively. The differential flux quantities for the three other 1ES 1101–232 epochs can be calculated using the ratios of the integral fluxes reported in Table 4.

7. Conclusions

HESS observed a large sample of AGN between January 2005 and July 2007 as part of a campaign to identify new VHE-bright AGN. Results presented here detail the observations of 14 candidates for which no significant excess was found. The corresponding upper limits on the VHE flux are the most stringent to date for eight of the candidates, and are only surpassed by those from earlier HESS observations (Aharonian et al. 2005d) for the other six candidates. In addition the results from HESS observations of four AGN known to emit VHE γ -rays are presented. Although only a marginal excess is measured for two of these objects, and no excess is observed from the other two, the presence of simultaneous X-ray data for three of these objects enables more accurate SED modeling than possible with archival data.

With the detection of ten VHE AGN, including the discovery of seven, the HESS AGN observation program has been highly successful. However, despite more than five years of operation, the observation program is not complete as many proposed

candidates have either not yet been observed or only have a fraction of their intended exposure. Therefore, the prospects of finding additional VHE-bright AGN with HESS are still excellent.

Acknowledgements. The support of the Namibian authorities and of the University of Namibia in facilitating the construction and operation of HESS is gratefully acknowledged, as is the support by the German Ministry for Education and Research (BMBF), the Max Planck Society, the French Ministry for Research, the CNRS-IN2P3 and the Astroparticle Interdisciplinary Programme of the CNRS, the UK Science and Technology Facilities Council (STFC), the IPNP of the Charles University, the Polish Ministry of Science and Higher Education, the South African Department of Science and Technology and National Research Foundation, and by the University of Namibia. We appreciate the excellent work of the technical support staff in Berlin, Durham, Hamburg, Heidelberg, Palaiseau, Paris, Saclay, and in Namibia in the construction and operation of the equipment. This research has made use of the SIMBAD database, operated at CDS, Strasbourg, France. This research has also made use of the NASA/IPAC Extragalactic Database (NED) which is operated by the Jet Propulsion Laboratory, California Institute of Technology, under contract with the National Aeronautics and Space Administration.

References

- Aharonian, F., Akhperjanian, A., Beilicke, M., et al. (HEGRA Collaboration) 2002, *A&A*, 393, 89
- Aharonian, F., Akhperjanian, A., Beilicke, M., et al. (HEGRA Collaboration) 2003, *A&A*, 403, L1
- Aharonian, F., Akhperjanian, A. G., Aye, K.-M., et al. (HESS Collaboration) 2004, *Astropart. Phys.*, 22, 109
- Aharonian, F., Akhperjanian, A. G., Aye, K.-M., et al. (HESS Collaboration) 2005a, *A&A*, 430, 865
- Aharonian, F., Akhperjanian, A. G., Aye, K.-M., et al. (HESS Collaboration) 2005b, *A&A*, 436, L17
- Aharonian, F., Akhperjanian, A. G., Aye, K.-M., et al. (HESS Collaboration) 2005c, *A&A*, 437, 95
- Aharonian, F., Akhperjanian, A. G., Bazer-Bachi, A. R., et al. (HESS Collaboration) 2005d, *A&A*, 441, 465
- Aharonian, F., Akhperjanian, A. G., Bazer-Bachi, A. R., et al. (HESS Collaboration) 2006a, *A&A*, 448, L19
- Aharonian, F., Akhperjanian, A. G., Bazer-Bachi, A. R., et al. (HESS Collaboration) 2006b, *Nature*, 440, 1018
- Aharonian, F., Akhperjanian, A. G., Bazer-Bachi, A. R., et al. (HESS Collaboration) 2006c, *A&A*, 455, 461
- Aharonian, F., Akhperjanian, A. G., Bazer-Bachi, A. R., et al. (HESS Collaboration) 2006d, *A&A*, 457, 899

- Aharonian, F., Akhperjanian, A. G., Bazer-Bachi, A. R., et al. (HESS Collaboration) 2006e, *Science*, 314, 1424
- Aharonian, F., Akhperjanian, A. G., Bazer-Bachi, A. R., et al. (HESS Collaboration) 2007a, *A&A*, 470, 475
- Aharonian, F., Akhperjanian, A. G., Bazer-Bachi, A. R., et al. (HESS Collaboration) 2007b, *ApJ*, 664, L71
- Aharonian, F., Akhperjanian, A. G., Barres de Almeida, U., et al. (HESS Collaboration) 2007c, *A&A*, 473, L25
- Aharonian, F., Akhperjanian, A. G., Barres de Almeida, U., et al. (HESS Collaboration) 2007d, *A&A*, 475, L9
- Albert, J., Aliu, E., Anderhub, H., et al. 2006, *ApJ*, 642, L119
- Albert, J., Aliu, E., Anderhub, H., et al. 2007, *ApJ*, 666, L17
- Benbow, W. 2005, *Proceedings of Towards a Network of Atmospheric Cherenkov Detectors VII* (Palaiseau), 163
- Berge, D., Funk, S., & Hinton, J. 2007, *A&A*, 466, 1219
- Bradbury, S. M., Deckers, T., Petry, D., et al. 1997, *A&A*, 320, L5
- Costamante, L., & Ghisellini G. 2002, *A&A*, 384, 56
- Feldman, G. J., & Cousins, R. D. 1998, *Phys. Rev. D*, 57, 3873
- Genzel, R., Weitzel, L., Tacconi-Garman, L. E., et al. 1995, *ApJ*, 444, 129
- Gould, R. J., & Schröder, G. P. 1967, *Phys. Rev.*, 155, 1408
- Hartman, R. C., Bertsch, D. L., Bloom, S. D., et al. 1999, *ApJS*, 123, 79
- Hauser, M. G., & Dwek, E. 2001, *ARA&A*, 39, 249
- Hinton, J. 2004, *New Astron. Rev.*, 48, 331
- Komossa, S., Voges, W., Xu, D., et al. 2006, *AJ*, 132, 531
- Li, T., & Ma, Y. 1983, *ApJ*, 272, 317
- Madau, P., & Pozzetti, L., 2000, *MNRAS*, 312, L9
- Mazin, D., Goebel, F., Horns, D., et al. 2005, *Proceedings of the 29th ICRC* (Pune), 4, 331
- Mitsuda, K., Bautz, M., Inoue, H., et al. 2007, *PASJ*, 59, 1
- Mukherjee, R., Bertsch, D. L., Bloom, S. D., et al. 1997, *ApJ*, 490, 116
- Padovani, P., & Giommi, P. 1995, *ApJ*, 444, 567
- Perley, R. A., Röser, H.-J., Meisenheimer, K., et al. 1997, *A&A*, 328, 12
- Perlman, E. S. 1999, *AIP Conf. Proc.*, 515, 53
- Primack, J. R., Bullock, J. S., & Somerville, R. S. 2005, *AIP Conf. Proc.*, 745, 23
- Punch, M., Akerlof, C. W., Cawley, M. F., et al. 1992, *Nature*, 358, 477
- Quinn, J., Akerlof, C. W., Biller, S. D., et al., 1996, *ApJ*, 456, L83
- Sowards-Emmerd, D., Romani, R. W., & Michelson, P. F. 2003, *ApJ*, 590, 109
- Superina, G., Benbow, W., Boutelier, T., et al. 2007, *Proceedings of the 30th ICRC* (Merida), in press
- Stecker, F. W., de Jager, O. C., & Salamon, M. H. 1996, *ApJ*, 473, L75
- Urry, C. M., & Padovani, P. 1995, *PASP*, 107, 803
- ⁶ LUTH, Observatoire de Paris, CNRS, Université Paris Diderot, 5 place Jules Janssen, 92190 Meudon, France
- ⁷ DAPNIA/DSM/CEA, CE Saclay, 91191 Gif-sur-Yvette, Cedex, France
- ⁸ University of Durham, Department of Physics, South Road, Durham DH1 3LE, UK
- ⁹ Unit for Space Physics, North-West University, Potchefstroom 2520, South Africa
- ¹⁰ Laboratoire Leprince-Ringuet, École Polytechnique, CNRS/IN2P3, 91128 Palaiseau, France
- ¹¹ Laboratoire d'Annecy-le-Vieux de Physique des Particules, CNRS/IN2P3, 9 chemin de Bellevue, BP 110, 74941 Annecy-le-Vieux Cedex, France
- ¹² Astroparticule et Cosmologie (APC), CNRS, Université Paris 7 Denis Diderot, 10 rue Alice Domon et Léonie Duquet, 75205 Paris Cedex 13, France UMR 7164 (CNRS, Université Paris VII, CEA, Observatoire de Paris)
- ¹³ Dublin Institute for Advanced Studies, 5 Merrion Square, Dublin 2, Ireland
- ¹⁴ Landessternwarte, Universität Heidelberg, Königstuhl, 69117 Heidelberg, Germany
- ¹⁵ Laboratoire de Physique Théorique et Astroparticules, CNRS/IN2P3, Université Montpellier II, CC 70, Place Eugène Bataillon, 34095 Montpellier Cedex 5, France
- ¹⁶ Universität Erlangen-Nürnberg, Physikalisches Institut, Erwin-Rommel-Str. 1, 91058 Erlangen, Germany
- ¹⁷ Laboratoire d'Astrophysique de Grenoble, INSU/CNRS, Université Joseph Fourier, BP 53, 38041 Grenoble Cedex 9, France
- ¹⁸ Institut für Astronomie und Astrophysik, Universität Tübingen, Sand 1, 72076 Tübingen, Germany
- ¹⁹ LPNHE, Université Pierre et Marie Curie Paris 6, Université Denis Diderot Paris 7, CNRS/IN2P3, 4 place Jussieu, 75252 Paris Cedex 5, France
- ²⁰ Institute of Particle and Nuclear Physics, Charles University, V Holesovickach 2, 180 00 Prague 8, Czech Republic
- ²¹ Institut für Theoretische Physik, Lehrstuhl IV: Weltraum und Astrophysik, Ruhr-Universität Bochum, 44780 Bochum, Germany
- ²² University of Namibia, Private Bag 13301, Windhoek, Namibia
- ²³ Obserwatorium Astronomiczne, Uniwersytet Jagielloński, Kraków, Poland
- ²⁴ Nicolaus Copernicus Astronomical Center, Warsaw, Poland
- ²⁵ School of Physics & Astronomy, University of Leeds, Leeds LS2 9JT, UK
- ²⁶ School of Chemistry & Physics, University of Adelaide, Adelaide 5005, Australia
- ²⁷ Toruń Centre for Astronomy, Nicolaus Copernicus University, Toruń, Poland
- ²⁸ European Associated Laboratory for Gamma-Ray Astronomy, jointly supported by CNRS and MPG

¹ Max-Planck-Institut für Kernphysik, PO Box 103980, 69029 Heidelberg, Germany
e-mail: Wystan.Benbow@mpi-hd.mpg.de

² Yerevan Physics Institute, 2 Alikhanian Brothers St., 375036 Yerevan, Armenia

³ Centre d'Étude Spatiale des Rayonnements, CNRS/UPS, 9 Av. du Colonel Roche, BP 4346, 31029 Toulouse Cedex 4, France

⁴ Universität Hamburg, Institut für Experimentalphysik, Luruper Chaussee 149, 22761 Hamburg, Germany

⁵ Institut für Physik, Humboldt-Universität zu Berlin, Newtonstr. 15, 12489 Berlin, Germany